Photochemical & Photobiological Sciences (2022) 21:373–384
https://doi.org/10.1007/s43630-022-00178-3

ORIGINAL PAPERS

Updated analysis of data from Palmer Station, Antarctica (64° S), and San Diego, California (32° N), confirms large effect of the Antarctic ozone hole on UV radiation

Germar H. Bernhard[1] · **Richard L. McKenzie**[2] · **Kathleen Lantz**[3] · **Scott Stierle**[3,4]

Received: 10 November 2021 / Accepted: 25 January 2022 / Published online: 23 February 2022

Abstract
The status of the stratospheric ozone layer is assessed by a panel of experts every 4 years. Reports prepared by this panel include a section with common questions and answers (Q&A) about ozone depletion and related matters. Since 2002, this Q&A supplement has featured a plot comparing historical and current ultraviolet (UV) Index data from Palmer Station, Antarctica (64° S), with measurements at San Diego, California (32° N), and Barrow, Alaska (79° N). The assumptions in generating these plots are discussed and an updated version is presented. The revised plot uses additional data up to the year 2020 and the methods used to create it are better defined and substantiated compared to those used for the legacy plot. Differences between the old and new UV Index values are small (typically < 5%). Both versions illustrate that the ozone hole has led to a large increase in the UV Index at Palmer Station. Between mid-September and mid-November, the maximum UV Index at this site has more than doubled compared to the pre-ozone-hole era (i.e., prior to 1980). When Palmer Station was below the ozone hole in December 1998, an "extreme" UV Index of 14 was observed, exceeding the highest UV Index of 12 ever measured at San Diego despite the city's subtropical latitude. Increases in the UV Index at Barrow and San Diego remain below 40% and 3%, respectively.

✉ Germar H. Bernhard
bernhard@biospherical.com

[1] Biospherical Instruments Inc., San Diego, CA, USA

[2] National Institute of Water and Atmospheric Research, Lauder, Central Otago, New Zealand

[3] NOAA Global Monitoring Laboratory, Boulder, CO, USA

[4] Cooperative Institute for Research in Environmental Sciences (CIRES), University of Colorado, Boulder, CO, USA

Graphical abstract

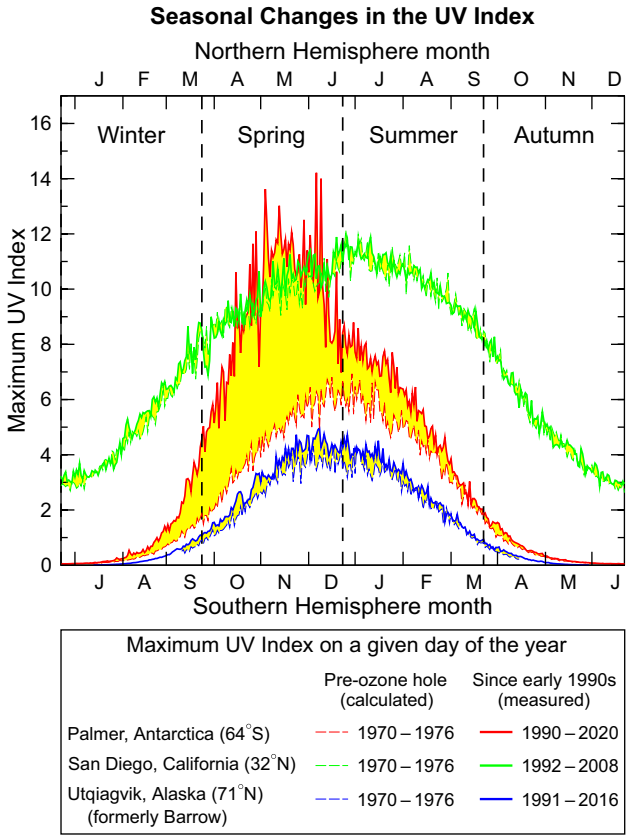

Keywords Ozone hole · Antarctica · UV radiation · Radiative transfer · Montreal protocol

1 Background and introduction

The Montreal Protocol on Substances that Deplete the Ozone Layer [1] includes a provision to regularly convene panels of experts for assessing the effectiveness of this important international treaty. One of these panels is the Scientific Assessment Panel (SAP). Every 4 years, the SAP prepares a comprehensive report on the status of the ozone layer and relevant atmospheric science issues.[1] Since 1994 [2], these reports have included a section on common questions and answers (Q&A) about the ozone layer for specialists and non-specialists alike. This first Q&A document included the question[2] "Is the depletion of the ozone layer leading to an increase in ground-level ultraviolet radiation?" and noted that "because of the ozone hole, the UV-B intensity at Palmer Station, Antarctica, in late October, 1993, was more intense than found at San Diego, California, at any time during all of 1993." Q&A sections of subsequent assessment reports continued to include comparisons of ultraviolet (UV) radiation measurements at Palmer Station, Antarctica (64° S), and San Diego, California (32° N). These discussions of geographical differences in UV radiation grew more sophisticated over time. The Q&A section of the 2002 assessment report [3] included for the first time a plot comparing modeled UV data for Palmer Station ("Palmer" hereafter) for a period prior to the formation of the Antarctic ozone hole (when no direct UV radiation measurements are available) with UV data measured between 1991 and 2001 when the ozone hole was well established. These data were also contrasted with UV measurements from San Diego and Barrow (recently renamed to Utqiaġvik), Alaska (71° N), to provide a comparison with UV levels at low and high northern latitudes, respectively. The plot was updated for the 2010 assessment report [4] to include data up to 2006 and is shown in Fig. 1. The same plot was also used for the assessment reports of 2014 and 2018 [5, 6].

[1] All reports prepared by the SAP can be downloaded at https://csl.noaa.gov/assessments/ozone.

[2] The document is available at https://csl.noaa.gov/assessments/ozone/1994/commonquestions7.html

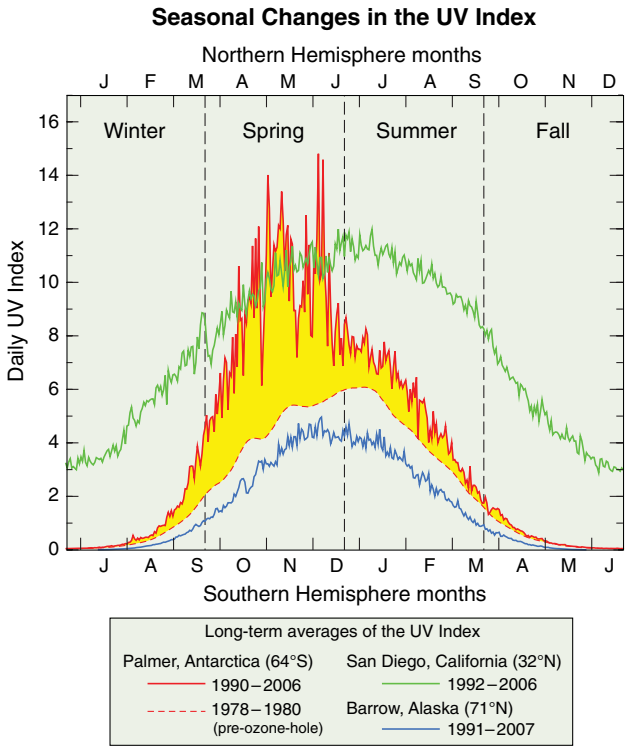

Fig. 1 Seasonal changes in the UV Index (UVI) as presented in the Q&A sections of the Scientific Assessments of Ozone Depletion: 2010, 2014, and 2018 [4–6]. The highest UVIs ever measured for each day of the year at Palmer, San Diego, and Barrow after 1990 are compared with the reconstructed UVI at Palmer for the pre-ozone-hole period 1978–1980. The difference in the UVI at Palmer between 1978–1980 and 1990–2006 (indicated by yellow shading) illustrates the effect of Antarctic ozone depletion, which is particularly strong during spring. The highest UVIs observed at Palmer during the more recent period exceed measurements at San Diego despite the city's much lower latitude. (The figure is in the public domain and may be reused with proper attribution to the source [6])

UV radiation is quantified with the dimensionless UV Index (or UVI), which measures the intensity of UV radiation in terms of causing erythema (sunburn) in human skin [7]. The UVI is calculated by weighting solar UV spectra with the action spectrum of erythema [8] and scaling the result with 40 m^2/W.

The plot shown in Fig. 1 has several shortcomings:

- The plot includes measurements only up to 2006 at Palmer and San Diego, and up to 2007 at Barrow, and is now dated.
- Reconstructed data for Palmer are based on the *average* total ozone column (TOC) observed between 1978 and 1980 by the Total Ozone Mapping Spectrometer (TOMS) onboard NASA's Nimbus-7 satellite. Analysis presented in Sect. 2.2.1 suggests that some ozone depletion was already present during this period. In addition, the use of the average TOC leads to a bias in the reconstructed UVI, because the *highest* historical UVI should be associated with the *lowest* ozone measurements during the pre-ozone-hole era. The period 1978–1980 is also too short for obtaining good statistics on the historical TOC.
- The effect of clouds in the historical Palmer dataset was assumed to be identical with that in the more recent data (1990–2006). To assess cloud effects, measured spectra from the years 1990–2006 were compared with spectra calculated with the radiative transfer model UVSPEC/libRadtran [9] assuming clear skies. Measured and modeled spectra were then integrated over the wavelength interval 337.5–342.5 nm and the ratio of measured and modeled irradiances was used for quantifying cloud effects. Reconstructed data shown in Fig. 1 are based on the 90th percentiles of the distribution of cloud attenuation obtained from the ratios of measured and modeled irradiances and are identical with the upper envelope of the historical range shown in Fig. 3.4a by Bernhard et al. [10]. Because of the use of the 90th percentiles instead of the distribution's maxima, this reconstruction likely underestimates the actual historical UVI maxima slightly.
- The measured UVI at Palmer shows a strong day-to-day variability due to short-term fluctuations in TOC and cloudiness while the historical dataset is unrealistically smooth.
- Reconstructed historical data for San Diego and Barrow are not included.
- The legend is mislabeled. The plot does not show "Long-term averages of the UV Index". Instead, it shows the highest UVI ever observed at the three stations during the periods indicated.

Because of the limitations of the plot used in the last reports, it was decided to update the plot for the Q&A section of the 2022 assessment report, which is being prepared as of this writing.

The objective of this paper is to describe the datasets and methods used for creating an updated version of the plot shown in Fig. 1. The new plot is based on all available UV measurements from the three sites, provides a more accurate reconstruction of UVIs for the historical period at Palmer, and includes reconstructions for San Diego and Barrow. Specifically, the effect of clouds is better represented and historical TOC data are based on measurements by the Backscatter Ultraviolet (BUV) experiment on the Nimbus-4 satellite between 1970 (start of BUV measurements) and 1976. Analysis presented below suggests that the ozone hole had not yet developed during this period.

2 Data

2.1 UV radiation measurements

UV Index data were calculated from UV spectra measured by SUV-100 spectroradiometers at Palmer (1990–2020), San Diego (1992–2008), and Barrow (1991–2016). Up to 2008, the instruments were part of the National Science Foundation's (NSF) UV Monitoring Network [11]. Thereafter, the instrument at Palmer became part of the Antarctic UV Monitoring Network of the National Oceanic and Atmospheric Administration (https://gml.noaa.gov/grad/antuv/). Between 2009 and until its decommissioning in 2016, the instrument at Barrow was integrated into the Arctic Observing Network initiated by the NSF. Quality-controlled measurements of the instrument at San Diego are only available until April 2008.

Data from Palmer and Barrow are based on the "Version 2" data edition [12] and have been corrected for the irradiance collector's cosine error [13], consistently aligned in wavelength against the Fraunhofer structure in a reference solar spectrum, and normalized to a spectral bandwidth of 1.0 nm. The uncertainty (95% confidence interval) of the UVI calculated from these spectral measurements varies between 5.6 and 6.6% at both sites, depending on solar zenith angle and sky condition [14, 15]. Both instruments are part of the Network for the Detection of Atmospheric Composition Change (NDACC; www.ndacc.org; [16]) and meet the criteria for NDACC UV measurements [17]. Version 2 data from Palmer have recently been examined for irregularities in calibrations that may have occurred between 1996 and 2020 [18]. For most years, calibrations were accurate to within ± 2%, but some solar data measured between 1997 and 1999 were found to be too high by 3–4%. Data from Palmer used for the updated Q&A plot were corrected by scaling with the "Method 3" factors that are listed in Table 1 by Bernhard et al. [18].

The SUV-100 spectroradiometer at San Diego is of the same type as the instruments at Palmer and Barrow and uses the same entrance optics. Identical quality control protocols have been implemented for the three instruments [19]. However, Version 2 data are not available and measurements at San Diego are, therefore, biased low because of the missing cosine error correction. At Palmer, this correction increases UVI measurements on average by 4.1% ± 2.0% (± 1σ). Measurements at San Diego were scaled up by 4.1% to be more consistent with measurements at Palmer. This simple scaling is adequate for the illustrative Q&A plot, considering that the dependence of the correction on solar zenith angle, clouds, the irradiance collector's cosine error, and other factors is within about ± 3%.

2.2 Total ozone column data

2.2.1 Total ozone column at Palmer

TOC data from Palmer for the period of UV measurements were derived from measurements of the SUV-100 spectroradiometer with an inversion algorithm described by Bernhard et al. [20]. These data agree with measurements of TOMS Nimbus-7 performed between March 1990 and May 1993 to within 1% [15].

TOC data from the pre-ozone-hole period 1970–1976 are based on BUV Nimbus-4 overpass data for Palmer, available at https://acd-ext.gsfc.nasa.gov/Data_services/merged/index.html.[3] These data are part of the SBUV[4] Merged Ozone Data Set (MOD), which includes measurements from many SBUV instruments installed on different satellites. SBUV TOC data from 1990 to 1993 were compared against the SUV-100 TOC dataset and found to be biased low by 1.6%. BUV data were scaled up by 1.6% to be more consistent with recent data. However, this adjustment is uncertain considering that the BUV instrument used during the 1970–1976 period is different from the SBUV radiometer that was operational between 1990 and 1993. According to the SBUV MOD website, "remaining offsets (mostly sub 5% levels) between [SBUV] instruments exist, but their cause is not understood. We, therefore, do not make adjustments to the data." Validation of BUV Nimbus-4 TOC data against the ground-based Dobson network suggests that BUV data are biased low by 9.5 DU or approximately 3% [21].

Figure 2 shows (1) available BUV Nimbus-4 TOCs for the period 1970–1976 (panel a), (2) TOMS Nimbus-7 TOCs for the period 1978–1980 (panel b), and (3) TOCs from the SUV-100 measurements for the period 1990–2020 (panel c). (1) is the pre-ozone-hole period considered for the new Q&A plot, (2) is the pre-ozone-hole period used for the Q&A plot of the last three ozone assessment reports, and (3) is the period of the ozone hole era for which also UV radiation measurement exist. Each panel includes all available data (red dots), the minima for each Day of Year (DOY) (blue circles), and an approximating spline-fit to these minima. These smooth functions will be used for the reconstruction of the historical UVIs (Sect. 3). Figure 2d compares the fit functions of the three periods. The fit to the BUV data has generally the largest TOCs and shows little variation with DOY. In comparison, the fit to TOMS data of 1978–1980 is 20 DU (6%) lower on average, and the largest difference is observed in September and early October when the ozone hole of the last 30 years has been the deepest.

[3] Overpass file: https://acd-ext.gsfc.nasa.gov/anonftp/toms/sbuv/MERGED/sbuv_v86.mod_r7.v8_lyr.palmer_292.txt

[4] Solar Backscatter Ultraviolet Radiometer.

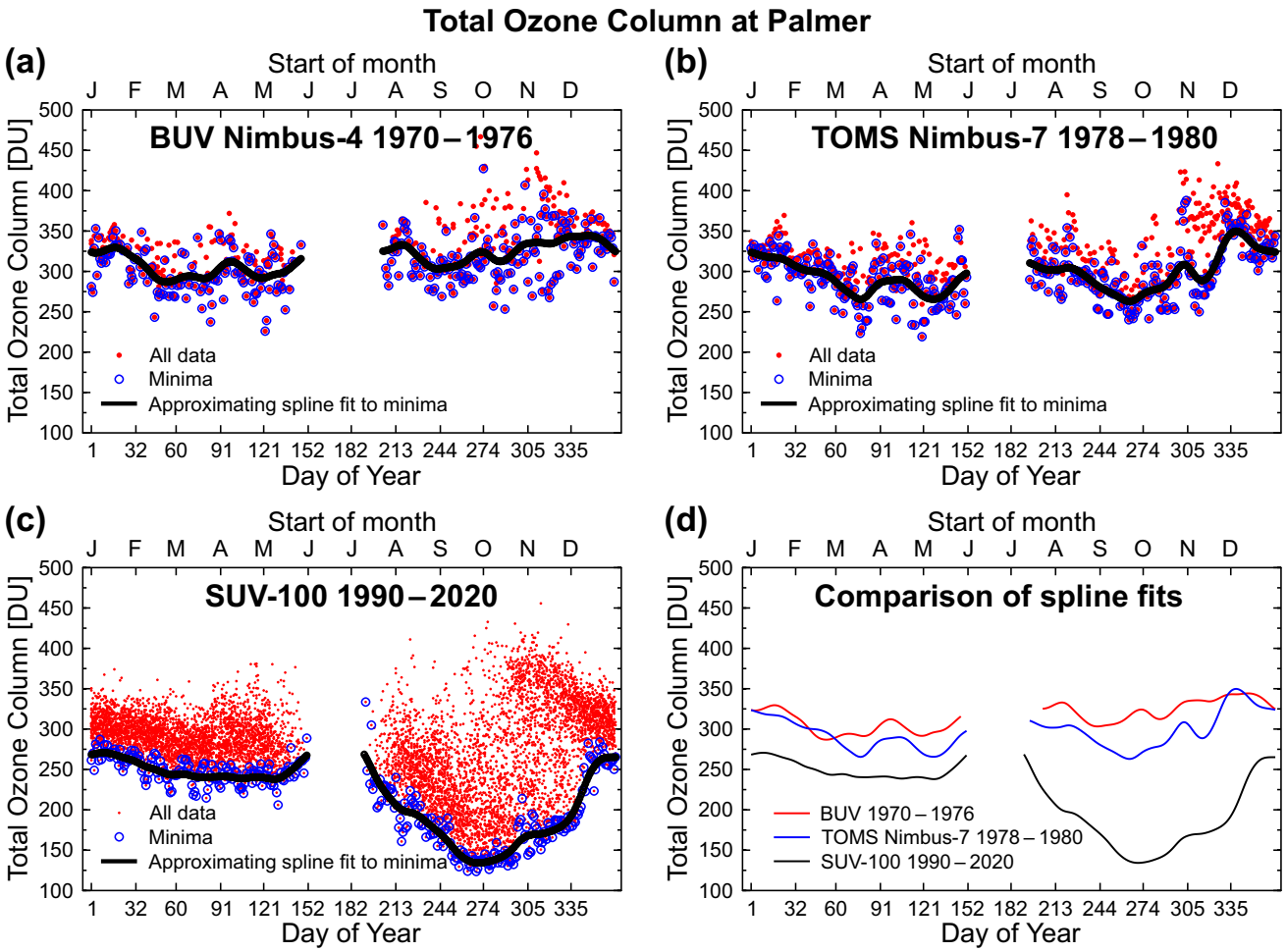

Fig. 2 Total ozone column at Palmer. **a** BUV Nimbus-4 TOC for the period 1970–1976, **b** TOMS Nimbus-7 TOC for the period 1978–1980, **c** SUV-100 TOC for the period 1990–2020, and **d** approximating spline fits to TOC minima of panels **a**–**c**. Panels **a**–**c** show all available data (red dots), minima for each DOY (blue circles), and approximating spline fits to these minima (black lines)

This is consistent with the assumption that there was already some ozone depletion between 1978 and 1980. Lastly, the fit curve for 1990–2020 has the lowest TOC values of the three datasets and shows strong ozone depletion between August and mid-December with an overall minimum of 134 DU. (For comparison, minima for the 1970–1976 and 1978–1980 periods are 287 and 263 DU, respectively.)

2.2.2 Total ozone column at Barrow

Data sources of TOCs at Barrow are identical to those for Palmer. Specifically, pre-ozone depletion (1970–1976) TOC data for Barrow are based on BUV Nimbus-4 overpass data and TOC data for the period of UV measurements (1991–2016) were derived from measurements of the SUV-100 spectroradiometer at Barrow. SUV-100 data exceed SBUV data by 0.7% on average, and BUV data were scaled by this amount for consistency. Figure 3 shows TOCs for the two periods. As for Palmer, the figure includes all available data, the minima for each DOY, and approximating spline-fit to these minima, which are subsequently used in Sect. 3 for reconstructing historical UVIs. Minima for the later period (1991–2016) are lower than those for the earlier period (1970–1976) by 15 to 25% for March and April, 10 to 20% between May and September, and 20 to 25% for October. These differences are much smaller than those observed at Palmer (Fig. 2d).

3 Data analysis

In this section, the highest daily maximum UVIs ever measured at Palmer and Barrow are compared with corresponding modeled UVIs. After confirming that these modeled values agree on average with the measurements, the model is used for the reconstruction of pre-ozone-hole UVIs utilizing BUV

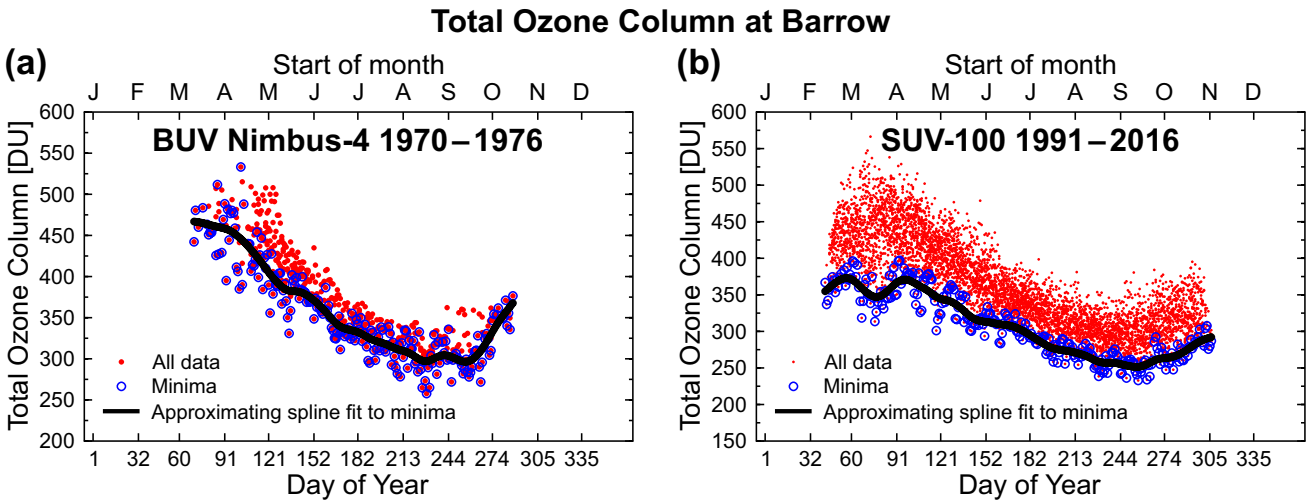

Fig. 3 Total ozone column at Barrow. **a** BUV Nimbus-4 TOC for the period 1970–1976 and **b** SUV-100 TOC for the period 1991–2016. Both panel show all available data (red dots), minima for each DOY (blue circles), and approximating spline fits to these minima (black lines)

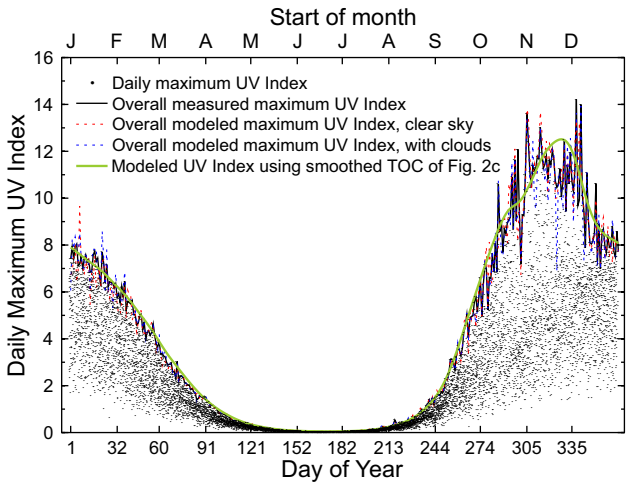

Fig. 4 Daily maximum UVI at Palmer for the period 1990–2020. Black dots show the daily maximum UVI for all days in this period. The black line is the upper envelope of these daily maxima, indicating the highest UVI measured on each DOY. The red broken line indicates the modeled Version 2 clear-sky UVI. The blue broken line is the same dataset scaled with the factor defined in Eq. (1). The green line is the modeled clear-sky UVI using the splined (smoothed) TOC dataset shown in Fig. 2c

Nimbus-4 TOC data from 1970–1976. The effect of clouds is subsequently added with a statistical method as the timing of the actual historical cloud cover is not known.

3.1 Data analysis for Palmer

Figure 4 shows the daily measured and modeled UVI maxima at Palmer for all days of the 31-year period from 1990 to 2020 (black dots—up to 31 for each day). There is a large day-to-day variability, reflecting large variations in TOC and cloud effects. The black line is the upper envelope of these daily maxima, indicating the highest UVI for each DOY. The red broken line indicates clear-sky UVIs modeled with UVSPEC/libRadtran [9]. Modelling takes the actual TOC, ozone profile, and surface albedo into account. The model implementation is described by Bernhard et al. [12] and input parameters specific to Palmer are discussed by Bernhard et al. [15]. Measured and modeled UVI data plus input parameters for every modeled spectrum are part of the Version 2 dataset and are available at http://uv.biospherical.com/ (up to 2009) and https://gml.noaa.gov/grad/antuv/ (from 2009).

Note that attenuation or enhancement by clouds has not yet been considered. To include cloud effects, the modeled clear-sky UVI was scaled with the ratio of measured and modeled irradiances at 340 nm, which are also available from the Version 2 dataset:

$$\widehat{E}_C(\mathrm{UVI}) = E_C(\mathrm{UVI}) \times \frac{E_M(340)}{E_C(340)}, \tag{1}$$

where $\widehat{E}_C(\mathrm{UVI})$ is the modeled UVI corrected for cloud effects, $E_C(\mathrm{UVI})$ is the Version 2 clear-sky model UVI, $E_M(340)$ is the measured spectral irradiance integrated over the wavelength interval 337.5–342.5 nm, and $E_C(340)$ is the corresponding modeled irradiance. UV irradiances in this wavelength range depend very little on ozone and can therefore be used to quantify the influence of clouds, independent of ozone. The scaling further assumes that the effects of clouds on the UVI and on the irradiance at 340 nm are comparable. This assumption is reasonable because attenuation by clouds has typically a weak wavelength dependence

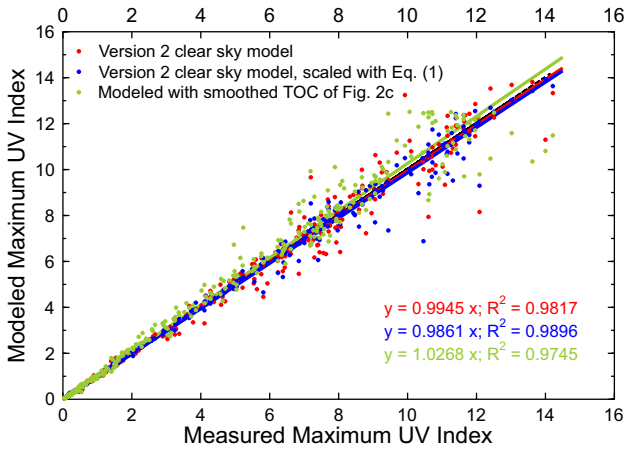

Fig. 5 Scatter plot of modeled UVI (y-axis) and measured maximum UVI (x-axis). Regression equations and coefficient of determination (R^2) are indicated in matching colors

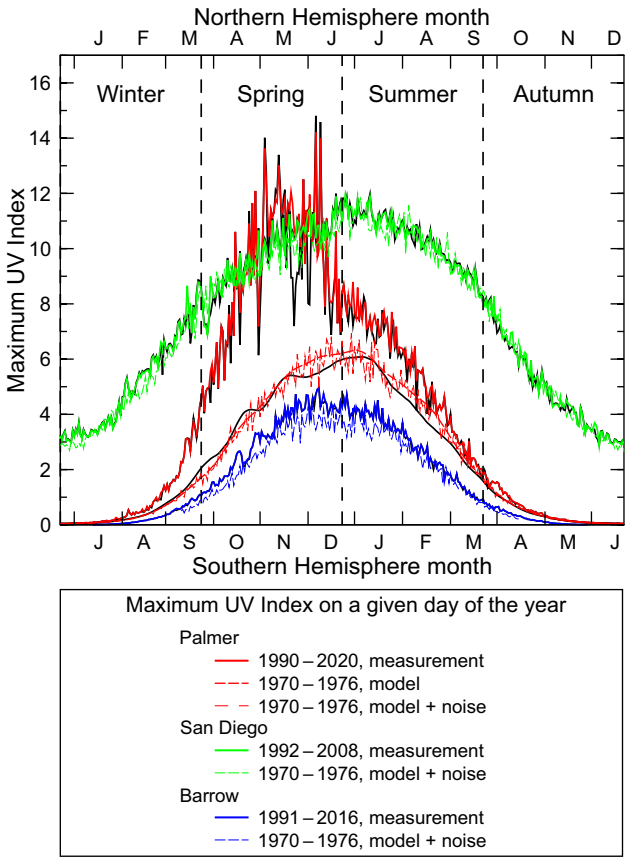

Fig. 6 Comparison of updated UVI data (colored lines) with legacy data plotted in Fig. 7 (black lines). Reconstructed data for Palmer are shown with and without the addition of noise, which indicates the approximate range of day-to-day variability in pre-ozone hole data

between 300 and 340 nm [22], i.e., the wavelength range mostly responsible for erythema [8].

The green line in Fig. 4 is the modeled clear-sky UVI using the splined (smoothed) TOC dataset shown in Fig. 2c. Other modeling parameters, including surface albedo, are based on the climatological average.

Figure 4 suggests that measured and modeled UVI maxima agree reasonably well. (For obvious reasons, the UVI dataset that uses the smoothed TOC data of Fig. 2c cannot resolve day-to-day fluctuations.) However, it is difficult to quantitatively compare measured and modeled data from this figure. To better discern these differences, modeled data were plotted as a function of the measurements (Fig. 5). Regression lines fitted to these datasets indicate very little ($<\pm 3\%$) bias between model and measurements for the three model runs.

The coefficients of determination R^2 are larger than 0.974 for the three datasets. The modeled dataset that is corrected for cloud effects (blue) is generally not in better agreement[5] with the measured data than the clear-sky model (red). This somewhat surprising finding can be explained with variations in the radiation field during the period of 2.5 min that it takes for the SUV-100 spectroradiometer to scan between 300 to 340 nm. In particular during periods of broken clouds, which can enhance measurements above the clear-sky limit and hereby leading to some of the largest UVIs of the time series, variations in excess of $\pm 20\%$ are sometimes observed at Palmer within this short time interval (e.g., Fig. 6 by Bernhard et al. [15]). While the model run that is based on the smoothed ozone dataset (green data in Fig. 5) has the largest bias (2.7%) and lowest R^2 (0.9745) of the three simulations, the agreement with the measurement is still remarkably good. Hence, the good agreement between measurement and model derived from the smoothed TOC data of 1990–2020 suggests that the maximum UVIs of the pre-ozone-hole period can be estimated with reasonable accuracy by using the smoothed TOC data of the 1970–1976 period shown in Fig. 2a as input to the model.

The relative standard deviation of the ratio of the measured and modeled UVIs using the smoothed ozone dataset (green data in Fig. 4) is 11.1% for September to December (months affected by the ozone hole) and 6.6% for January to April. The larger variability during the "ozone hole months" can be expected because of the dynamics of the ozone hole. For example, Palmer is frequently moving in and out of the ozone hole area during these months, resulting in large changes. Before the development of the ozone hole in the 1980s, the year-round UVI variability was likely closer to the variability that is now observed between January and April, and a relative standard deviation of 7% seems

[5] While the dataset that is corrected for cloud effects has a slightly larger (better) R^2 value than the clear-sky dataset, the slope of the regression line is marginally closer to unity for the clear-sky data.

reasonable for characterizing the variability for all seasons. Hence, to account for day-to-day variations in the simulated UVI of the pre-ozone-hole period, reconstructed clear-sky data based on the smoothed BUV TOC values were multiplied with normally-distributed random numbers with a mean of 1 and a standard deviation of 0.07. In the absence of actual historical cloud data, this method provides a visual clue in the updated Q&A plot of the variability in the UVI that has likely occurred in the past. Of course, the simulated locations of highs and lows do not match those of the actual (but unknown) historical time series.

3.2 Data analysis for Barrow

Data from Barrow were analyzed in the same way as those from Palmer and only a brief summary of the results is provided here. Model input parameters specific to Barrow are discussed by [14]. Measured UVI data from 1991 to 2016 were regressed against (a) modeled clear-sky data that are part of the Version 2 dataset and (b) UVIs modelled using the splined TOC dataset shown in Fig. 3b plus climatological averages for all other input parameters (e.g., surface albedo, aerosols, ozone profile). The bias between model and measurement is 0.1% for model run (a) and 5.1% for model run (b); R^2 is 0.9915 for run (a) and 0.9857 for run (b). The relative standard deviation of the ratio of the measured and modeled UVIs is 8%.

The excellent agreement for run (a) confirms that the factors affecting UV radiation at Barrow are well understood. The larger bias of 5.1% for run (b) can still be considered acceptable considering that this value is smaller than the uncertainties of the measurements and the uncertainties arising from the use of climatological data, in particular albedo.

Historical UVIs for 1970–1976 were calculated by repeating model run (b) with the splined TOC BUV dataset shown in Fig. 3a. No correction for the bias of 5.1% was applied because the reason for this discrepancy could not be determined. Hence, these reconstructed UVIs have an uncertainty of approximately the same magnitude. To account for day-to-day variations, reconstructed clear-sky data were multiplied with normally distributed random numbers with a standard deviation of 0.08, similar to the approach taken for Palmer.

3.3 Data analysis for San Diego

As Version 2 data for San Diego are not available, we were not able to validate model calculations with measurements as we have done for Palmer and Barrow. Historical UVIs for 1970–1976 were reconstructed using BUV overpass TOC data, which were processed in the same way as BUV data for Palmer and Barrow. These calculations assumed a time-invariant surface albedo of 3% and an aerosol optical depth of 0.18 at 310 nm estimated from nearby (La Jolla) Aerosol Robotic Network (AERONET; https://aeronet.gsfc.nasa.gov) measurements. Clear-sky model data were multiplied with normally distributed random numbers with a standard deviation of 0.04, which was estimated from the day-to-day variation of maximum UVIs measured between 1992 and 2008.

4 Results

Figure 6 compares the updated datasets (colored lines) with the data plotted in Fig. 1 (black lines). Overall, the updated datasets are very similar to data used for the Q&A plot published in the last assessment report [6], but several differences can be discerned:

- Measured maximum UVIs at Palmer for 1990–2006 (Fig. 1 and black line in Fig. 6) show a large drop at the end of October and also include a period of relatively low UVI values between the middle and end of the November. As data from 2007 to 2020 were added for the updated plot (red line in Fig. 6), these periods of low UVI measurements are "filled in". For example, the deep and long-lasting ozone hole of 2020 [23] led to new UVI maxima on 24, 28, and 29 November. The UVI observed on 29 November 2020 was 12.0 and replaced the previous UVI maximum of this day of 8.0; an increase by 50%.
- The correction that was recently applied to Palmer data [18] led to small changes in UVI maxima. For example, the two overall maxima (UVIs of 14.8 and 14.6 observed on 4 and 7 December 1998) were reduced by 4% to 14.2 and 14.0, respectively.
- The cosine error correction of San Diego was reduced from 5 to 4.1% for the updated version. Updated UVIs for San Diego are therefore smaller by 0.9% on average. As two additional years of data were added, the updated dataset is slightly smoother than that used for the previous version.
- The overall maximum UVI at San Diego is 11.9, which is 2.3 UVI units below the overall maximum UVI of 14.2 at Palmer. This result may be counterintuitive considering that San Diego is located at a subtropical latitude of 32°, which is exactly half the latitude of Palmer. Because the Sun's elevation above the horizon is one of the most important determinants of the UVI, sites with low latitude (and thus high solar elevation) have typically higher UVIs than high-latitude locations. However, this is not the case here because UVI enhancements resulting from low TOCs under the ozone hole at Palmer (e.g., Fig. 2c) outweigh the Sun-angle effect.
- Even though nine additional years of data were added to the dataset for Barrow, maximum UVIs of the two ver-

sions are virtually identical. Maximum UVIs at Barrow are considerable smaller than those at Palmer because of Barrow's higher latitude and naturally occurring higher TOCs with less spring-time ozone depletion in the Arctic compared to Antarctica [6].

- Reconstructed data for Palmer of the old and new version (without noise added) are similar despite the different methods used for these estimates. Between mid-September and the end of October, updated UVIs are slightly smaller because BUV Nimbus-4 TOC data used for the new plot are larger than TOMS Nimbus-7 data utilized for the legacy plot. Between mid-November and mid-March, the legacy dataset tends to be smaller than the new data, because it was based on the 90th percentile in cloud attenuation, whereas the updated dataset is based on clear-sky modeling. Cloud effects were considered by adding noise to the modeled data as described in Sect. 3 and are indicated by the jagged red line in Fig. 6.
- Ozone depletion has led to large increases in the UVI at Palmer year-round, with the largest increases occurring during spring, the season most affected by the ozone hole. Between 15 September and 15 November, the maximum UVI at this site is now larger by a factor of 2.50 ± 0.37 ($\pm 1\sigma$) on average compared to the pre-ozone-hole period. During summer and autumn (21 December—21 June), i.e., the seasons least affected by the ozone hole, UVIs maxima measured between 1990 and 2020 exceed maxima estimated for years prior to 1976 by $20\% \pm 13\%$. This increase is consistent with the decrease in the TOC shown in Fig. 2d. We note that these enhancements are subject to uncertainty, because historical UVIs at Palmer were not directly measured and are based on the assumption that surface albedo and attenuation by clouds and aerosols have not changed over the last 50 years.
- Reconstructed UVI data for San Diego and Barrow that were similarly calculated from BUV TOCs of 1970–1976 are also included in Fig. 6. At San Diego, measured and reconstructed data are almost indistinguishable. On average, the UVI increased by $3 \pm 7\%$ ($\pm 1\sigma$), since the 1970s. This small change is within the uncertainties of the measurements and model calculations, and is consistent with the conclusion that maximum daily UVI values have remained essentially constant at mid-latitudes over the last ~ 20 years, thanks to the phase-out of ozone depleting substances regulated by the Montreal Protocol [24]. At Barrow, the UVI increased by $18 \pm 15\%$ ($\pm 1\sigma$) since the 1970s, which is beyond the combined uncertainties of measurements and modeling. The largest spikes in the UVI of up to 40% relative to the 1970s were measured during spring in years with abnormally strong Arctic ozone depletion such as 2011 [25]. While these changes are much larger compared to San Diego, they are still small compared with those at Palmer, because spring-time ozone depletion is much smaller in the Arctic compared to the Antarctic [6].

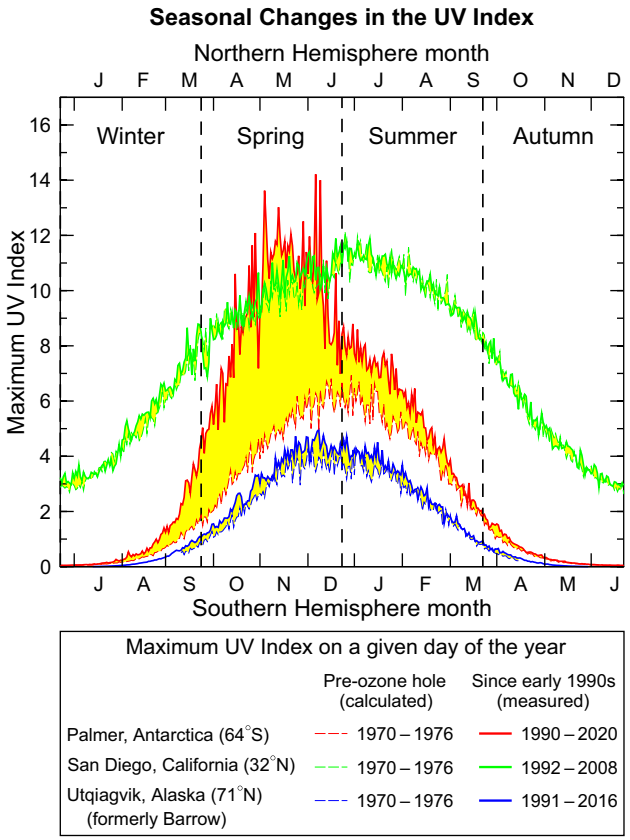

Fig. 7 Same as Fig. 1 but updated for Q&A supplement of the "Scientific Assessment of Ozone Depletion: 2022" report, which is being prepared as of this writing. The dataset for Barrow is labeled "Utqiaġvik (formerly Barrow)" as the town of Barrow was recently renamed. Yellow shading indicates changes between reconstructed pre-ozone hole UVIs and UVIs measured since the earlier 1990s

5 Discussion and conclusions

Since 2002, the Q&A sections of Scientific Assessments of Ozone Depletion reports [3–6] have featured a plot comparing historical and current maximum UVIs at Palmer with measured UVIs at San Diego and Barrow. In this paper, limitations of this plot were discussed and the datasets and methods for producing an updated and improved version were presented. Figure 7 shows the new plot, which is proposed for use in the next edition of the Q&A supplement complementing the "Scientific Assessments of Ozone Depletion: 2022" report, which is being prepared as of this writing.

The updated plot is similar to the legacy plot but is based on longer time series (in particular at Palmer and Barrow), uses an updated dataset for Palmer, a slightly modified

cosine error correction for San Diego, employs an improved method for reconstructing UVIs at Palmer for the pre-ozone-hole period, and also includes UVI reconstructions for San Diego and Barrow. The new results confirm the previous conclusion that the ozone hole led to large UVI enhancements at Palmer Station: between mid-September and mid-November, UVI maxima appear to have more than doubled compared to the pre-ozone-hole era and now occasionally exceed UVI maxima at San Diego.

A similar increase in UVI maxima by approximately a factor of two relative to the pre-ozone-hole era has also been reported for McMurdo Station (78° S) and South Pole (90° S) [10]. Both sites also use SUV-100 spectroradiometers and are part of the same UV monitoring network as Palmer. The highest UVIs measured between 1990 and 2020 at McMurdo Station and South Pole are 7.7 and 4.1, respectively. These values are much smaller than the all-time UVI maximum of 14.2 measured at Palmer. This large difference can be explained by the higher latitudes of McMurdo Station and South Pole compared to Palmer, and the resulting lower solar elevations. Hence, the observation that UVIs at Antarctica can exceed UVIs of subtropical sites such as San Diego only applies to locations at the perimeter of the Antarctic continent.

There are no reliable data describing long-term changes in effective surface albedo and cloudiness at Palmer. For the reconstruction of historical UVIs, we, therefore, assumed that albedo and cloud cover at this site have not changed between 1970 and 2020. While changes in these two parameters may have occurred (for example, due to climate change), the effect on the UVI can be considered small (e.g., $< 5\%$) compared to the increase in UVI caused by ozone depletion.

Unfortunately, data for San Diego are available only until 2008. However, UV radiation at this latitude has likely not changed since the last 13 years [24] and the dataset for San Diego would likely change very little if such data could be included. This assertion is also supported by the observation that reconstructed UVIs at San Diego for 1970–1976 agree within the measurement uncertainty with measurements performed between 1992 and 2008. The conclusion that UVI values have remained essentially constant over the last ~ 20 years [24] even extends to Barrow where maximum UVIs for 1991–2006 (legacy plot) and 1991–2016 (revised plot) are virtually identical, with the exception of a few days that are filled-in with larger values, leading to a somewhat smoother curve in Fig. 7. However, the UVI at Barrow has changed by $18 \pm 15\%$ ($\pm 1\sigma$) between the 1970s and the early 1990s before the effect of the Montreal Protocol became apparent, as the comparison with reconstructed data indicates. It is likely that new UVI maxima occurred at Barrow in March 2020 when the Arctic was affected by exceptionally large ozone depletion [26]. Unfortunately, there are no UVI measurements available to confirm this.

Random numbers for describing day-to-day variations in the reconstructed UVI datasets cannot describe the precise timing of actual highs and lows of the past but are useful for illustrating the approximate range of variability. Overall, the various datasets are better described and should be more accurate than the datasets used in the legacy plot. In particular, the basis of the reconstructed data for Palmer used in the updated plot is better defined and substantiated. Since measurements of UV radiation and cloud attenuation data prior to the development of the ozone hole do not exist, these reconstructed data form the best available foundation for the comparison with contemporary data.

Acknowledgements We are grateful to numerous instrument operators for their dedicated work in acquiring high-quality UV data at Palmer, San Diego, and Barrow, and to Vi V. Quang of BSI for help in data processing. We also thank two anonymous reviewers for their valuable comments.

Author contributions GHB performed the analyses and wrote the paper. RLM motivated this study and contributed to writing this manuscript. KL is overseeing the operation of NOAA's Antarctic UV Monitoring Network and contributed to writing this manuscript. SS serviced and calibrated the instrument at Palmer Station and prepared the raw data. All authors have read the manuscript and endorsed its submission to *Photochemical & Photobiological Sciences*.

Funding The NSF Ultraviolet Spectral Irradiance Monitoring Network (UVSIMN) was sponsored by the US National Science Foundation's Office of Polar Programs (Prime Contract Number OPP 0000373) and was operated by Biospherical Instruments Inc. (BSI) until 2008. The NOAA Antarctic UV Monitoring Network is funded by NOAA's Global Monitoring Laboratory. BSI has a sub-contract (contract number RA133R17SE0836P20003) from NOAA's Western Acquisition Division for processing data of the NOAA Antarctic UV Monitoring Network.

Data availability Data from the UVSIMN are available at http://uv.biospherical.com/; data from NOAA's Antarctic UV Monitoring Network are available at https://gml.noaa.gov/grad/antuv/.

Declarations

Conflict of interest The authors declare no financial interest beyond their benefits from employment.

References

1. United Nations. (1987). Montreal protocol on substances that deplete the Ozone Layer, *United Nations Treaty Series*, 1522. https://treaties.un.org/Pages/showDetails.aspx?objid=080000028003f7f7.
2. WMO. (1995). *Scientific Assessment of Ozone Depletion: 1994*. Global Ozone Research and Monitoring Project—Report No. 37, edited by D.L. Albritton, R.T. Watson, and P.J. Aucamp, World Meteorological Organisation, Geneva, Switzerland.
3. WMO. (2003). *Scientific Assessment of Ozone Depletion: 2002*, Global Ozone Research and Monitoring Project—Report No. 47, edited by A.-L. Ajavon, D.L. Albritton, M. G., and R.T. Watson, p. 498, World Meteorological Organisation, Geneva, Switzerland.
4. WMO. (2011). *Scientific Assessment of Ozone Depletion: 2010*, Global Ozone Research and Monitoring Project—Report No. 52, edited by A.-L. Ajavon, P.A. Newman, J.A. Pyle, and A.R. Ravishankara, p. 516, World Meteorological Organisation, Geneva, Switzerland.
5. WMO. (2014). *Scientific Assessment of Ozone Depletion: 2014*, Global Ozone Research and Monitoring Project—Report No. 55, edited by A.-L.N. Ajavon, P.A. Newman, J.A. Pyle, and A.R. Ravishankara, p. 416, World Meteorological Organisation, Geneva, Switzerland.
6. WMO. (2018). *Scientific Assessment of Ozone Depletion: 2018*, Global Ozone Research and Monitoring Project—Report No. 58, edited by D.W. Fahey, P.A. Newman, J.A. Pyle, and B. Safari, p. 588, World Meteorological Organization, Geneva, Switzerland.
7. WHO. (2002). *Global solar UV Index: A practical guide*, 28 pp., World Health Organisation (WHO), World Meteorological Organisation (WMO), United Nations Environment Program (UNEP), and International Commission on Non-Ionising Radiation Protection (ICNRP), Geneva, Switzerland.
8. McKinlay, A. F., & Diffey, B. L. (1987). A reference action spectrum for ultra-violet induced erythema in human skin. In W. F. Passchier & B. F. M. Bosnajakovic (Eds.), *Human exposure to ultraviolet radiation: Risks and regulations* (pp. 83–87). Elsevier.
9. Mayer, B., & Kylling, A. (2005). Technical note: The libRadtran software package for radiative transfer calculations—description and examples of use. *Atmospheric Chemistry and Physics, 5*, 1855–1877. https://doi.org/10.5194/acp-5-1855-2005.
10. Bernhard, G., Booth, C., & Ehramjian, J. (2010). Climatology of ultraviolet radiation at high latitudes derived from measurements of the National Science Foundation's ultraviolet spectral irradiance monitoring network, in *UV Radiation in Global Climate Change*, edited by W. Gao, J. Slusser, and D. Schmoldt, pp. 48–72, Tsinghua University Press, Beijing and Springer, New York. https://doi.org/10.1007/978-3-642-03313-1_3.
11. Booth, C.R., Lucas, T.B., Morrow, J.H., Weiler, C.S., & Penhale, P.A. (1994). The United States National Science Foundation's polar network for monitoring ultraviolet radiation, in *Ultraviolet radiation in Antarctica: Measurements and biological effects*, edited by C.S. Weiler and P.A. Penhale, 62, pp. 17–37, American Geophysical Union, Washington, D.C. https://doi.org/10.1029/AR062p0017.
12. Bernhard, G., Booth, C. R., & Ehramjian, J. C. (2004). Version 2 data of the National Science Foundation's ultraviolet radiation monitoring network: South Pole. *Journal of Geophysical Research: Atmospheres, 109*(D21), D21207. https://doi.org/10.1029/2004jd004937.
13. Seckmeyer, G., & Bernhard, G. (1993). Cosine error correction of spectral UV-irradiances, in *Proc. SPIE, Atmospheric Radiation*, edited by K.H. Stamnes, 2049, pp. 140–151, SPIE, Bellingham, WA. https://doi.org/10.1117/12.163505.
14. Bernhard, G., Booth, C. R., Ehramjian, J. C., Stone, R., & Dutton, E. G. (2007). Ultraviolet and visible radiation at Barrow, Alaska: Climatology and influencing factors on the basis of version 2 National Science Foundation network data. *Journal of Geophysical Research: Atmospheres, 112*(D09101), 1–19. https://doi.org/10.1029/2006JD007865.
15. Bernhard, G., Booth, C.R., & Ehramjian, J.C. (2005). UV climatology at Palmer Station, Antarctica, based on version 2 NSF network data, in *Proc. SPIE, Ultraviolet Ground- and Space-based Measurements, Models, and Effects V*, edited by G. Bernhard, J.R. Slusser, J.R. Herman, and W. Gao, 5886, pp. 58860701–58860712, SPIE, Bellingham, WA. https://doi.org/10.1117/12.614172.
16. De Mazière, M., Thompson, A. M., Kurylo, M. J., Wild, J. D., Bernhard, G., Blumenstock, T., Braathen, G. O., Hannigan, J. W., Lambert, J.-C., Leblanc, T., McGee, T. J., Nedoluha, G., Petropavlovskikh, I., Seckmeyer, G., Simon, P. C., Steinbrecht, W., & Strahan, S. E. (2018). The network for the detection of atmospheric composition change (NDACC): History, status and perspectives. *Atmospheric Chemistry and Physics, 18*(7), 4935–4964. https://doi.org/10.5194/acp-18-4935-2018.
17. McKenzie, R.L., Johnston, P.V., & Seckmeyer, G. (1997), UV spectro-radiometry in the network for the detection of stratospheric change (NDSC), in *Solar Ultraviolet Radiation. Modelling, Measurements and Effects*, edited by C.S. Zerefos and A.F. Bais, 52, pp. 279–287, Springer-Verlag, Berlin. https://doi.org/10.1007/978-3-662-03375-3_21.
18. Bernhard, G., & Stierle, S. (2020). Trends of UV radiation in Antarctica. *Atmosphere, 11*(8), 795. https://doi.org/10.3390/atmos11080795.
19. Bernhard, G., Booth, C.R., Ehramjian, J.C., & Quang, V.V. (2008). *NSF Polar Programs UV Spectroradiometer Network 2006–2007 Operations Report, vol. 16.0*, Biospherical Instruments Inc, San Diego, CA, USA. http://uv.biospherical.com/report_0607/REPVOL16.pdf.
20. Bernhard, G., Booth, C. R., & McPeters, R. D. (2003). Calculation of total column ozone from global UV spectra at high latitudes. *Journal of Geophysical Research: Atmospheres, 108*(D17), 4532. https://doi.org/10.1029/2003JD003450.
21. Reinsel, G., Tiao, G. C., & Lewis, R. (1982). A statistical analysis of total ozone data from the Nimbus-4 BUV satellite experiment. *Journal of the Atmospheric Sciences, 39*(2), 418–430. https://doi.org/10.1175/1520-0469(1982)039%3c0418:ASAOTO%3e2.0.CO;2.
22. Seckmeyer, G., Erb, R., & Albold, A. (1996). Transmittance of a cloud is wavelength-dependent in the UV-range. *Geophysical Research Letters, 23*(20), 2753–2755. https://doi.org/10.1029/96GL02614.
23. Kramarova, N., Newman, P.A., Nash, E.R., Strahan, S.E., Long, C.S., Johnson, B., Pitts, M., Santee, M.L., Petropavlovskikh, I., Coy, L., de Laat, J., Bernhard, G.H., Stierle, S., & Lakkala, K. (2021). 2020 Antarctic ozone hole, in *"State of the Climate in 2020", Bulletin of the American Meteorological Society*, edited by J. Blunden and T. Boyer, 102(8), pp. S345–S349. https://doi.org/10.1175/BAMS-D-21-0081.1.
24. McKenzie, R., Bernhard, G., Liley, B., Disterhoft, P., Rhodes, S., Bais, A., Morgenstern, O., Newman, P., Oman, L., Brogniez, C., & Simic, S. (2019). Success of montreal protocol demonstrated by comparing high-quality UV measurements with "world avoided" calculations from two chemistry-climate models. *Scientific Reports, 9*(1), 12332. https://doi.org/10.1038/s41598-019-48625-z.
25. Bernhard, G., Dahlback, A., Fioletov, V., Heikkilä, A., Johnsen, B., Koskela, T., Lakkala, K., & Svendby, T. (2013). High levels of ultraviolet radiation observed by ground-based instruments below the 2011 Arctic ozone hole. *Atmospheric Chemistry*

and Physics, 13(21), 10573–10590. https://doi.org/10.5194/acp-13-10573-2013.

26. Bernhard, G. H., Fioletov, V. E., Grooß, J. U., Ialongo, I., Johnsen, B., Lakkala, K., Manney, G. L., Müller, R., & Svendby, T. (2020). Record-breaking increases in arctic solar ultraviolet radiation caused by exceptionally large ozone depletion in. *Geophysical Research Letters, 47*, e2020GL090844. https://doi.org/10.1029/2020gl090844.